JOM, Vol. 72, No. 6, 2020
https://doi.org/10.1007/s11837-020-04170-z

A Brief Review of Fly Ash as Reinforcement for Composites with Improved Mechanical and Tribological Properties

ASHISH K. KASAR,[1] NIKHIL GUPTA,[2] PRADEEP K. ROHATGI,[3] and PRADEEP L. MENEZES[1,4]

1.—Department of Mechanical Engineering, University of Nevada, Reno, Reno, NV 89557, USA. 2.—Department of Mechanical and Aerospace Engineering, New York University, Tandon School of Engineering, 6 MetroTech Center, Brooklyn, NY 11201, USA. 3.—Department of Materials Science and Engineering, University of Wisconsin-Milwaukee, Milwaukee, WI 53201, USA. 4.—e-mail: pmenezes@unr.edu

Fly ash (FA) is one of the particulate wastes generated during combustion of coal in thermal power plants. Around 110 million tons of FA is generated in the USA every year, and 60% of it is deposited in landfills. Utilization of FA can create value for this waste material and also help the environment. FA is essentially a mixture of metal oxides that can be used as a filler reinforcement in metal and polymer composites. FA as a filler material reduces the amount of metals and polymer, reducing embodied energy. Hollow FA particles, called cenospheres, can provide the advantage of low density in composites as well as higher hardness and strength. FA also reduces the coefficient of thermal expansion. This article provides a brief review to capture the state of the art on the mechanical and tribological behavior of composites reinforced with FA to identify the possible benefits of using this waste material. The corrosion performance of metal matrix FA composites is also explored. Future perspectives in this field are discussed based on the potential applications of FA-filled composites.

INTRODUCTION

The four major coal combustion products generated in coal-fired power plants are fly ash (FA), bottom ash, boiler ash, and flue gas desulphurization gypsum. FA forms about 40% of all the waste in coal combustion products.[1] FA is a fine residue captured from the flue gases using electrostatic precipitators or filter fabric collectors. According to the ASTM C618-19 standard,[2] FA can be classified into three classes based on chemical composition, as presented in Table I. The primary utilization of FA is in cement, which is nonhazardous.[3] The other applications of FA are soil stabilization, structural fill, mineral filler for asphalt roads, flowable fill, geopolymers, bricks, waste treatment, and reinforcement for composites. Due to the environmental hazards of FA, products that utilize FA are defined as green and environmentally friendly products.

One of the major concerns about composite materials is their cost. New ways of lowering the cost of composite materials can help in accelerating their adoption in engineering applications. The use of FA can provide several advantages. The low density of FA compared with that of the matrix material can help in reducing the structural weight without the loss of mechanical properties. Lighter products can help in reducing the lifecycle cost in transportation applications. In addition, FA is a waste material that is available for free, compared with expensive engineered reinforcement materials. Figure 1 shows the cost of common reinforcement materials retrieved from US Research Nanomaterials, Inc.,[4] where FA is much cheaper (5–10 US¢/kg) or sometimes even presents a negative cost (a user may be paid for FA disposal). Most of the cost of FA is attributed to transportation and cleaning of the as-received material. Use of FA as reinforcement can reduce the cost of the composite material. These advantages have motivated investigating the properties of FA-filled composites in recent years.

Transportation applications of lightweight materials are very attractive for material saving and lowering of the lifecycle cost of the vehicle; For

(Published online April 21, 2020)

Table I. Chemical composition of three classes of FA

Chemical compound (%)	Class N	Class F	Class C
$SiO_2 + Al_2O_3 + Fe_2O_3$	70	50	50
CaO	Negligible (report only)	18 (maximum)	> 18
SO_3	4	5	5
Moisture	3	3	3

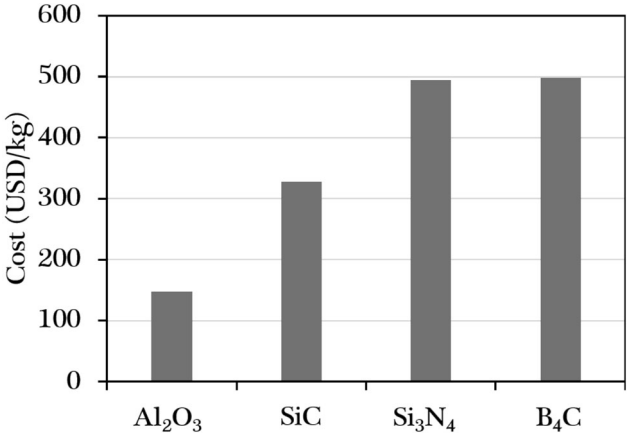

Fig. 1. The cost of materials commonly used as reinforcements. Although the cost may change significantly, the two orders of magnitude difference between the cost of reinforcement and matrix alloy is a significant factor that can be mitigated by using low-cost reinforcements such as fly ash

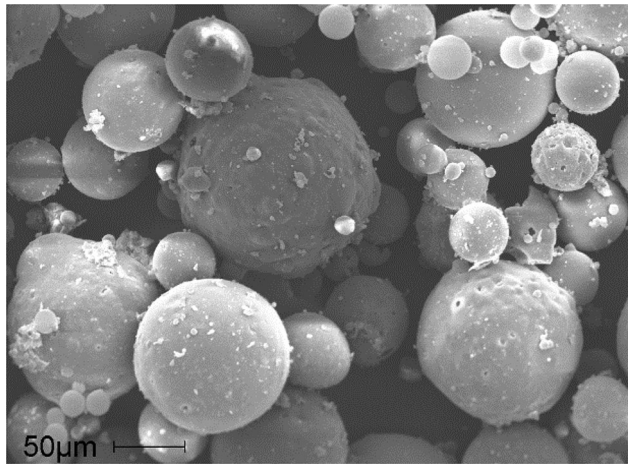

Fig. 2. A representative sample of FA showing hollow particles, called cenospheres, in a 10–100 μm size range

example, materials used in brakes are composed of both organic and inorganic, including metals, minerals, cellulose, glass, and rubber. The major constituents for the brake material are binder, fibrous reinforcement, filler materials, sliding materials, and friction modifiers.[5] Abrasive materials such as $A1_2O_3$, SiO_2, Fe_2O_3, and ZnO are used to control the frictional behavior. The filler and abrasive materials in the brake pad and brake linings can range between 15 vol.% and 60 vol.%. With 1.2 billion vehicles already in service, a number that is expected to rise to 2 billion by 2035, this one application itself can lead to substantial utilization of FA.[6] Strategic usage of waste materials such as FA for the brake components in the automotive industry would be economically as well as environmentally beneficial. Reduction in the use of primary metals by filling them with FA can be attractive. Rohatgi et al.[7] discussed that incorporation of 20 wt.% FA in aluminum (Al) matrix can save 38.86 kWh of energy for each kilogram of finished Al casting. Replacement of 10% Al used in the automotive industry by FA/Al composite can result in a total 92.25×10^6 kWh of energy saving.

In this review article, utilization of FA as reinforcement in metal and polymer matrices is discussed in relation to the resulting mechanical and tribological properties to assess the possibility of developing their industrial applications. The amount of literature published on FA composites is very large now, and covering all the studies in a single short review is impossible. Hence, a select few studies that show promising properties of FA-filled composites are used to develop the understanding of promises presented by these materials.

METAL MATRIX FA COMPOSITES

Mechanical Properties of Metal Matrix FA Composites

Al alloys are widely used in automotive and aerospace structures due to their low density and high specific strength. The performance of Al alloys has been further enhanced by the development of aluminum matrix composites (AMCs) reinforced with whiskers, fibers, and particles. The most common synthesis method for AMCs is the stir casting method due to its simplicity, low cost, and ability to distribute reinforcement uniformly in a wide range of volume fractions.[8,9] In addition, sand casting and infiltration methods have also been used to synthesize AMCs. The composition and hollow structure of FA particles present several specific challenges in synthesizing composites. A typical FA sample is shown in Fig. 2, which contains hollow particles, called cenospheres, of 10–100 μm

diameter. The hollow particles used in metal matrix composites (MMCs) typically have a density in the range of 500–900 kg/m^3. At this density level, they can provide a significant weight saving in metallic matrices.

Interfacial chemical reactions and formation of secondary phases during casting is a challenge because presence of brittle phases at the particle–matrix interface can result in poor mechanical properties. The presence of many chemical species in the FA particles makes it difficult to have complete control over the interfacial reactions because a large number of reactions are thermodynamically possible at the commonly used melt superheat temperature that is used for composite synthesis. The possible chemical reactions are shown in Eqs. 1–7 with the Gibbs free energy change (ΔG°) at 727°C [10,11]:

$$4Al_{(l)} + 3SiO_{2(s)} \leftrightarrow 3Si_{(s)} + 2Al_2O_{3(s)} \quad \left(\Delta G^\circ = -532.2 \text{ kJ mol}^{-1}\right) \tag{1}$$

$$2Al_{(l)} + Fe_2O_{3(s)} \leftrightarrow 2Fe_{(s)} + 2Al_2O_{3(s)} \quad \left(\Delta G^\circ = -799.6 \text{ kJ mol}^{-1}\right) \tag{2}$$

$$3Mg_{(l)} + 4Al_2O_{3(s)} \leftrightarrow 2Al_{(s)} + 3MgAl_2O_{4(s)} \quad \left(\Delta G^\circ = -215.1 \text{ kJ mol}^{-1}\right) \tag{3}$$

$$SiO_{2(s)} + 2Mg_{(l)} \leftrightarrow 2MgO_{(s)} + Si_{(s)} \quad \left(\Delta G^\circ = -255.6 \text{ kJ mol}^{-1}\right) \tag{4}$$

$$2SiO_{2(s)} + 2Al_{(l)} + Mg_{(l)} \leftrightarrow MgAl_2O_{4(s)} + 2Si_{(s)} \quad \left(\Delta G^\circ = -426.4 \text{ kJ mol}^{-1}\right) \tag{5}$$

$$3Mg_{(l)} + Fe_2O_{3(s)} \leftrightarrow 3MgO_{(s)} + 2Fe_{(s)} \quad \left(\Delta G^\circ = -917.0 \text{ kJ mol}^{-1}\right) \tag{6}$$

$$MgAl_2O_{4(s)} + 3Mg_{(l)} \leftrightarrow 4MgO_{(s)} + 2Al_{(s)} \quad \left(\Delta G^\circ = -84.9 \text{ kJ mol}^{-1}\right) \tag{7}$$

The negative ΔG° values suggests that the above reactions can occur spontaneously at 727°C in the Al melt. Understanding of these chemical reactions is crucial in the FA/Al composite because the release of elemental Si and Fe as a result of reaction between FA and Al can cause the formation of intermetallics. Some of the intermetallics are beneficial, such as $MgSi_2$, while some other intermetallics are brittle and undesired, such as Al_5FeSi and $Al_{15}(Fe,Mn)_3Si_2$, which can reduce the strength of AMCs.[12–14] However, the rates of formation of these reaction products are determined by kinetics, temperature, and reaction time.

Anilkumar et al.[15] investigated the mechanical properties of Al-6061 reinforced with FA of different particle sizes and composition synthesized using the stir casting method. AMCs containing 15 wt.% FA provided maximum ultimate tensile strength (UTS) compared with 10 wt.% and 20 wt.% FA-Al composites. Smaller FA particles (4–25 μm) yielded the highest UTS of $\sim$ 135 MPa compared with coarser FA particles (50 μm and 100 μm). Similar trends were also observed for hardness and compressive strength. The study suggested that, above 15 wt.% FA, there is a reduction in mechanical properties. In a similar study, Al 6061 was reinforced up to 12 wt.% FA, which resulted in a hardness value of 110 HV compared with 50 HV of Al 6061 alloy.[16] The UTS of Al composite was observed to increase by 50% compared with that of Al 6061 alloy. The study also confirmed by x-ray diffraction analysis that FA particles did not react with the melt.

In contradiction to these results, Gikunoo et al.[17] observed a decrease in hardness and tensile strength with the addition of FA in the A535 cast Al alloys. The composites of three different compositions were synthesized using the stir casting method: (1) hybrid composite with A 535 + 5 wt.% FA + 5 wt.% SiC, (2) A 535 + 10 wt.% FA, and (3) A 535 + 15 wt.% FA. The mean value of Vickers hardness number (VHN) of A 535 alloy was 170, which was reduced to $\sim$ 105 VHN with the addition of 15 wt.% FA. The study suggested that FA particles get attached to gas bubbles that lead to poor distribution and porosity, as shown in Fig. 3. It was observed that, due to the addition of 15 wt.% FA, the Mg concentration drastically decreased from 7.6 wt.% to 2 wt.%. However, the authors did not discuss the impact of lowering Mg concentration on the wettability of FA particles. Generally, lower Mg concentration causes reduced wettability and results in porosity or nonuniform distribution of reinforcement particles.[18]

Rohatgi et al.[19] incorporated up to 65 vol.% FA cenospheres into A356 matrix to synthesize MMCs using the pressure infiltration technique. Prior to casting, cenospheres were coated with ZrO_2 to avoid chemical reactions with Al melt. In the pressure infiltration technique, cenospheres were placed in a borosilicate glass tube, placed above the graphite crucible. Once the desired temperature was achieved for Al melt in a graphite crucible and cenospheres in the tube, the pressure was generated using nitrogen gas that caused the molten alloy to rise and fill the interparticle spacing. The authors prepared the composites with different cenosphere sizes and compositions. The observed stress–strain curves from compressive testing are shown in Fig. 4 for composites containing cenospheres of different

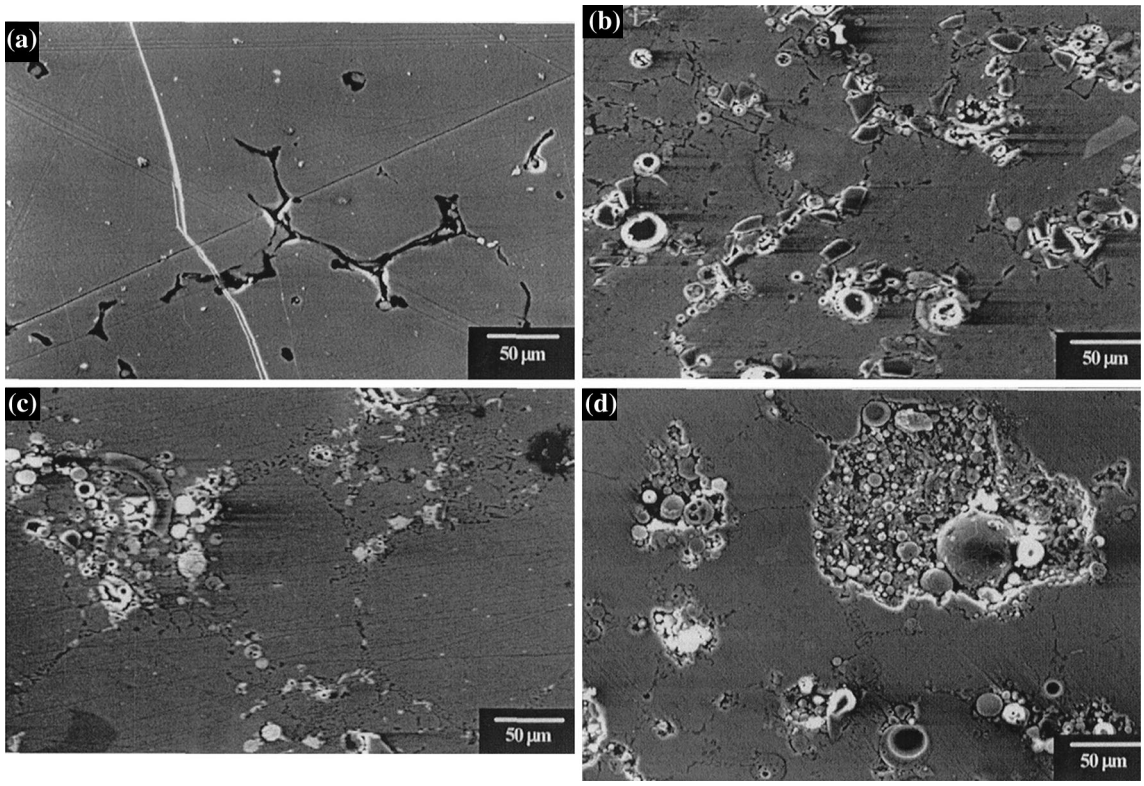

Fig. 3. Scanning electron microscopy (SEM) micrographs of (a) A535 alloy, (b) A535 hybrid, (c) A535-10 wt.% FA, and (d) A535-15 wt.% FA. Reprinted with permission from Ref. 17

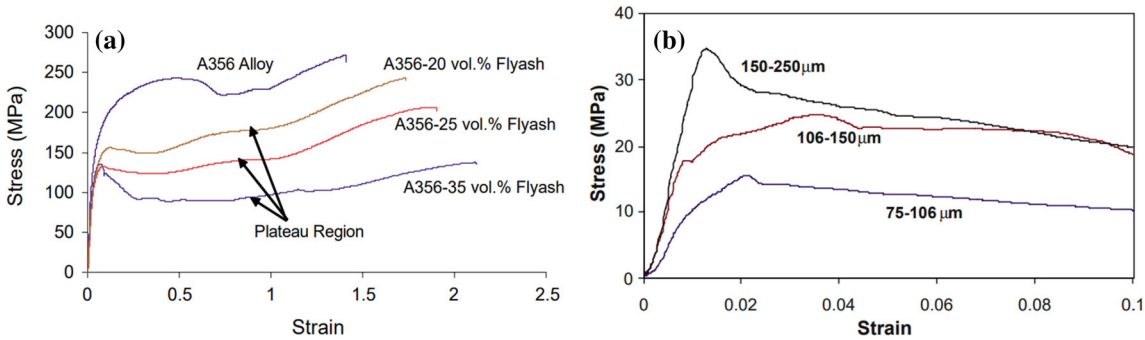

Fig. 4. Stress–strain curves for A356/FA cenosphere composites with variation in (a) FA content and (b) FA particle size. Reprinted with permission from Ref. 19

diameters in different volume fractions. Figure 4a shows the stress–strain curve for composites with different FA content that shows how the compressive yield strength decreases with increasing cenosphere content, likely due to the lower strength of cenospheres than that of the matrix. Figure 4b shows the stress–strain curve for composites containing 65 vol.% cenospheres of different diameters. The composite with bigger particles yielded maximum yield strength, and with decreasing particle size, yield strength decreases. The observed trend was due to the voids between the particles; higher void content was observed for the smaller particle size because of difficulty in infiltration of small interstitial spaces that ultimately reduces the strength.

The energy absorption capability of the Al alloys can be improved by incorporating cenospheres due to their porous structure. Luong et al.[20] studied the compressive properties of A4032 and A4032/cenosphere composites in the strain rate range of 0.003–2136 s^{-1}. The A4032 alloy did not show any measurable strain rate sensitivity in the tested strain rate range, whereas the yield strength of the composite showed strain rate sensitivity. At a low strain rate of 0.003 s^{-1}, the observed yield strength was 254 MPa, which increased to 288 MPa at a strain rate of 2136 s^{-1}. The study concluded that the severe deformation at high strain rates led to

crushing of cenospheres, which resulted in additional energy absorption capability in the composite. The higher energy absorption by A4032/cenosphere composite may enable their energy absorption applications. The same research group also studied the strain rate sensitivity in AZ91D alloys, which is a Mg-Al alloy.[21] The composites contained 5 wt.% cenospheres and were tested up to 1028 s^{-1} strain rate. The stress–strain curves for AZ91D alloy showed strain rate sensitivity due to the presence of hard intermetallic particles in the ductile Mg-Al matrix. The AZ91D/cenosphere composites also showed strain rate sensitivity in the compressive behavior. The results of mechanical properties are summarized in Fig. 5. At comparable strain rates, the cenosphere-filled composites have higher yield strength and elastic energy absorption capabilities than the matrix alloy. The improvement in the energy absorption is achieved while reducing the density by incorporation of cenospheres, which implies that the specific properties of the composite are substantially increased over the matrix alloy properties.

Juang et al.[22] used the friction stir processing on the Al alloy/5 wt.% cenosphere composite initially synthesized using the stir casting method. The study found that multipath friction stir processing causes squeezing and crushing of the cenospheres, reducing the particle size from a range of 53–106 μm to less than 10 μm, as shown in Fig. 6. Also, the particles redistributed more uniformly in the matrix. The friction stir processing also resulted in grain refinement of the aluminum alloy matrix by recrystallization. The combination of grain refinement and cenosphere particle size reduction increased the UTS and % elongation by 1.5 times and 2.6 times, respectively, compared with the as-cast samples.

Further enhancement in mechanical properties can be carried out by the development of hybrid composites containing cenospheres and an additional reinforcing phase in the MMC.[23,24] FA along with SiC has been found to improve tensile strength and hardness of Al 2024 alloy.[23] The maximum tensile strength (293 N/m^2) was observed for the composite with 10 wt.% FA and 10 wt.% SiC in Al 2024 matrix compared with 236 N/m^2 of the Al 2024 alloy. However, the elongation reduced from 19.4% to 11.9%. As the wettability can be an issue, the authors added 1.5 wt.% Mg to improve the wettability of SiC and FA during casting. Other studies with FA as reinforcement are listed in Table II, where properties are compared in percentage with respect to unreinforced alloy.

Tribological Properties of Metal Matrix FA Composites

MMCs with hard particles such as SiO_2, Al_2O_3, SiC, Si_3N_4, and other ceramic particles offer superior resistance to wear for the machine components. FA, being a combination of hard oxides, has proven to be a promising reinforcement for improving tribological properties. Ramachandra and Radhakrishna[25] studied the tribological properties of the Al-12.2Si alloy reinforced with 5 wt.%, 10 wt.%, and 15 wt.% FA. Wear tests were carried out against steel disc at different loads of 4.9 N, 9.8 N, and 14.7 N at a fixed velocity of 95 m/min. The study observed that the coefficient of friction (COF) reduced with the increase in the FA content. At 14.7 N load, the COF for Al-12.2Si alloy was around 0.4, which was reduced to 0.09 with addition of 15 wt.% FA. The wear behavior also showed a similar trend. The wear depth of base Al alloy after 8400 s was $\sim$ 1900 μm, which is significantly higher than the 1200 μm wear depth in case of 15 wt.% FA composite. After microscopic examination of wear tracks, several different mechanisms were proposed based on operating parameter and filler content, including

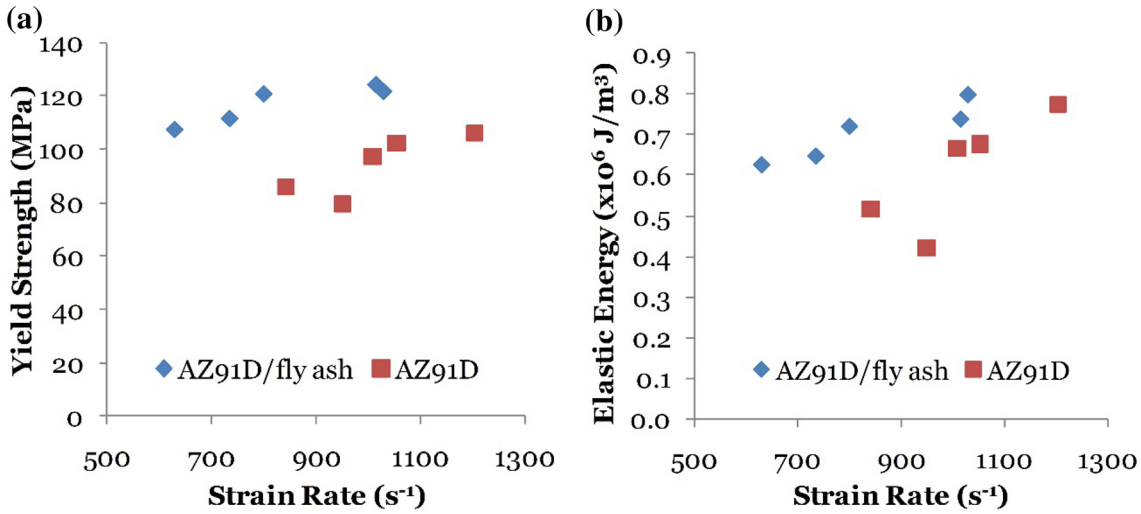

Fig. 5. Comparison of (a) yield strength and (b) elastic energy absorption in AZ91D alloy and AZ91D/cenosphere composites at various strain rates. Reprinted with permission from Ref. 21

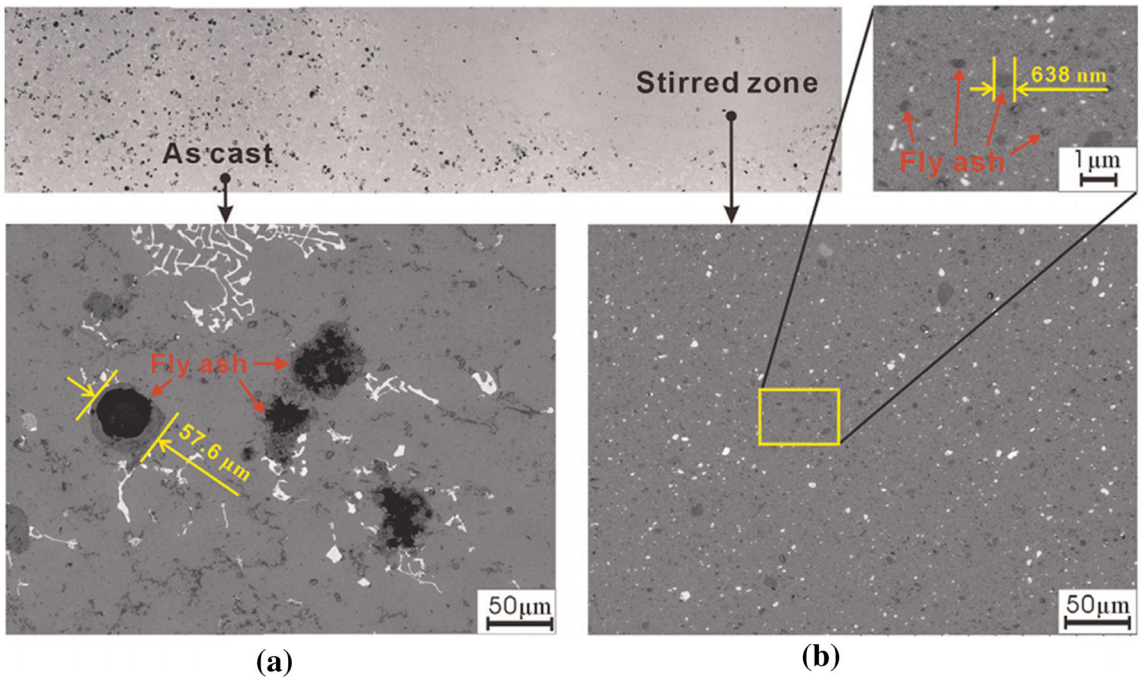

Fig. 6. SEM micrograph of (a) as-cast and (b) friction stir processed sample. Reprinted with permission from Ref. 22

Table II. Mechanical and tribological performance of FA metal matrix composites with different matrix and FA contents

Matrix	Reinforcement	Property[a]	References
Ni	FA = 40 vol.%	Hardness = 135%, COF = − 33%, Wear rate = − 63%	27
A 535	FA = 15 wt.%	TS = − 79%, Hardness = − 40%	17
Al-12.2Si	FA = 15 wt.%	COF = − 15%, Wear = − 37%	25
AA 2024	FA = 10 wt.%	Hardness = 73%	28
Al 6061	FA = 15 wt.%	UTS = 6.4%	15
AlSi10Mg	FA = 9 wt.% Graphite = 3 wt.%	Hardness = 20%, TS = 26%, COF = − 28%, Wear rate = − 80%	26
AA 6063	FA = 12 wt.%	Impact energy = − 58%, Hardness = 47%	29
AA 7075	FA = 12 wt.%	Hardness = 20.89%, UTS = 23%	30
A356	FA cenosphere = 35 vol.%	Compressive yield strength = − 36%	19
Pure Al	FA cenosphere = 64 vol.%	CTE = − 56% to −48%	31
AZ31D	FA cenosphere = 5 wt.%	Compressive yield strength = + 19–41% based on strain rate	21
ADC6	FA = 5 wt.%	UTS = − 40%	22
AA7075	TiO_2 = 10 wt.%, FA = 3 wt.%	Compressive strength = ∼ 100%	32
Al-7Si	FA = 6 wt.%	Hardness = 29%	33

COF Coefficient of friction, *UTS* ultimate tensile strength, *TS* tensile strength, *CTE* coefficient of thermal expansion[a]Properties compared with respect to unreinforced matrix; negative sign indicates decrease in property with respect to unreinforced matrix

abrasion, oxidation, delamination, thermal softening, and adhesion. Formation of grooves at all the test conditions confirmed the abrasion mechanism. In addition to abrasion, oxidation was also observed. Under 14.7 N and 95 m/min, delamination was observed on the composite with lower FA content, but delamination was replaced by thermal softening and adhesion at higher sliding velocity. Delamination and adhesive wear were reduced with higher FA content. Improvement in the tribological properties due to FA has also been observed in AlSi10Mg alloy filled with graphite particles.[26] The COF and wear rate at different loads for this material system are shown in Fig. 7a and b, respectively. It can be seen that addition of graphite reduced the COF and wear because of the lubrication effect, but COF and wear further reduced with addition of FA in the Al matrix due to the reinforcement effects. The

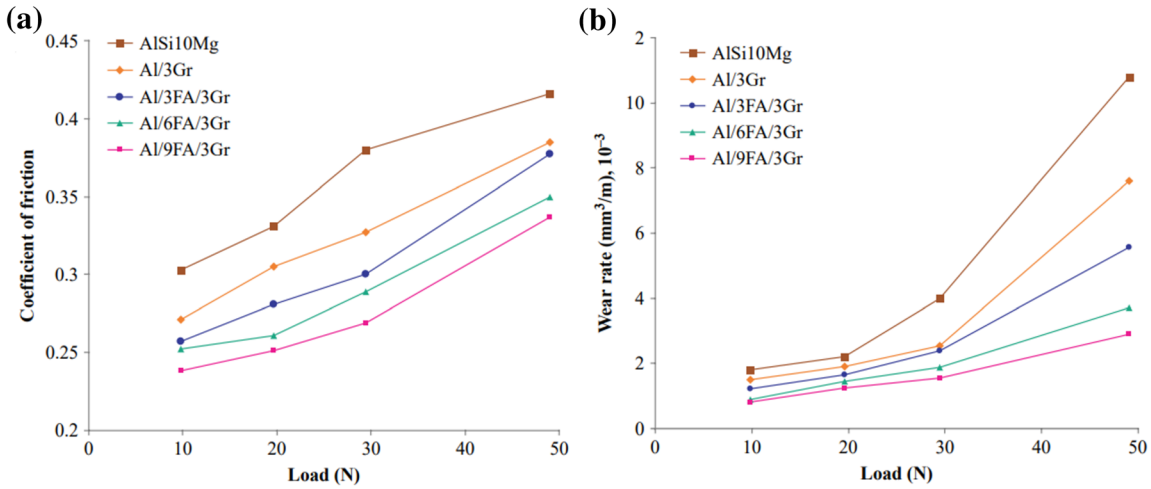

Fig. 7. Variation in (a) coefficient of friction and (b) wear rate with load for Al alloys and FA composites tested against EN-32 steel disc. Reprinted with permission from Ref. 26

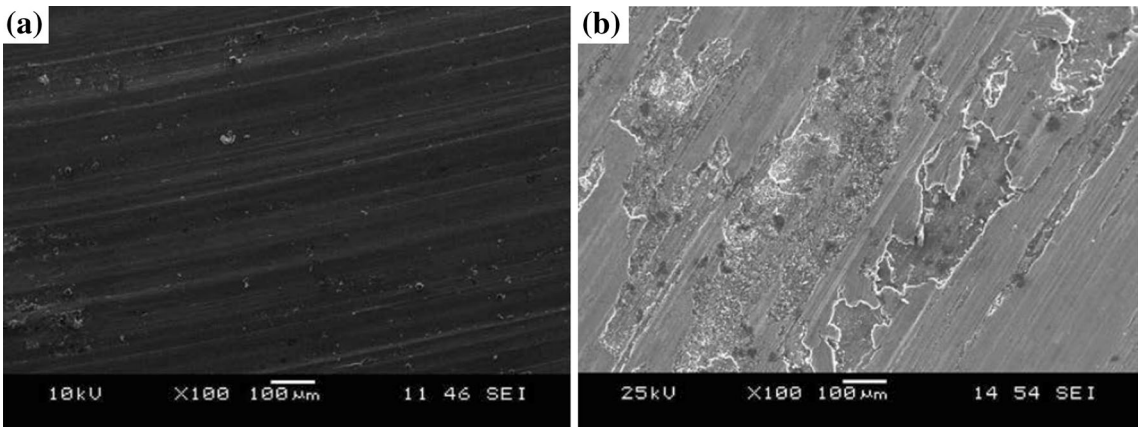

Fig. 8. Wear track on Al/9wt.%FA/3wt.% graphite composite at (a) 9.81 N and (b) 49.05 N. Reprinted with permission from Ref. 26

abrasive wear was observed at lower loads, whereas adhesive wear became dominant at higher loads. However, the transition load from abrasive to adhesive wear was much higher for the FA composites compared with the unreinforced Al alloy. Figure 8a shows the abrasive wear of Al/9 wt.% FA/3 wt.% graphite composite at 9.81 N with fine grooves that changes to adhesive wear at 49.05 N, as shown in Fig. 8b. Similar behavior was observed with several other MMCs, mainly AMCs, as summarized in Table II.

Corrosion Performance of FA Composites

Metals and alloys are susceptible to pitting corrosion due to the addition of alloying elements and reinforcement materials by creating internal galvanic pairs. The addition of FA in the Al matrix has been observed to increase pitting corrosion.[28,34] Bienia et al.[34] studied the corrosion behavior of the AK 12 (AlSi12CuNiMg)-9 wt.% FA composite prepared using the gravity and squeeze casting methods. Squeeze casting resulted in more uniform distribution of FA particles compared with gravity casting. Also, lesser porosity was observed on samples manufactured by the squeeze casting method. The authors investigated the gravity cast sample by the potentiodynamic and immersion tests in 3.5 wt.% NaCl aqueous solution for 50 days. The measured pitting potential of the AK 12 alloy (− 613 mV) was higher than that of the composite (− 640 mV); the lower potential of the composite indicates lower corrosion resistance. The immersion test and the potentiodynamic test results showed similar results: the weight loss after 50 days was higher for composite compared with the AK 12 alloy.

Similar corrosion behavior was observed for AA 2024-FA composite by Rao et al.[28] The authors measured the pitting potential in 3.5 wt.% NaCl of the composites with amounts of FA varying from 2% to 10%. The measured pitting potentials are tabulated in Table III. It can be observed that the pitting potentials for the composites are lower than those of

Table III. Pitting potential of AA 2024/FA composites

FA (wt.%)	E_{pit} (mV)
0%	− 576.75
2%	− 719.69
4%	− 621.52
6%	− 703.26
8%	− 722.1
10%	− 625.79

the AA 2024 alloy, which suggests higher pitting corrosion in the composites. The likely reason for this increase in corrosion is the formation of a discontinuous passive Al oxide layer over the FA particles and intermetallics. In addition, the FA particles can act as initiation sites for pitting.

CENOSPHERE-REINFORCED POLYMER MATRIX COMPOSITES

Mechanical and Tribological Properties

The density of most polymers is in the range of 0.9–1.2 g/cm^3. Incorporation of cenospheres with density less than 0.7 g/cm^3[35] results in lightweight polymer matrix composites (PMCs) for weight-sensitive applications similar to the use of cenospheres in MMCs.[36,37] However, achieving uniform distribution of cenospheres in PMCs is a challenging task due to poor wettability of FA with polymers. The cenosphere–polymer interaction can be improved by treating the cenosphere surface with appropriate agents. Silane treatment of reinforcement is conducted to make them compatible with a variety of resins.[38] In some cases, compatibilization of the resin system is also necessary to promote interfacial bonding between particles and the resin. However, some of these treatments result in lowering of the modulus of the resin system.[39] Kulkarni and Kishore[40] investigated the compressive properties of the 10 vol.% FA-epoxy composites after three different surface treatments of FA: (1) cleaning of FA surface with acetone, (2) exposure of the cleaned FA to paraffine oil, and (3) coating of FA particles with silane. The highest compressive strength of 118 MPa was observed for silane-coated FA/epoxy composite followed by paraffine-oil-modified FA/epoxy composite (108.9 MPa) and acetone-cleaned FA/epoxy (98.2 MPa). The untreated FA/epoxy composite provided only 94 MPa of compressive strength. These results show the importance of interfacial strength in defining the properties of a composite.

The other important consideration is the amount of FA content in the polymer matrix that should be optimized based on the required properties. Figure 9 shows the relative particle modulus plotted with respect to radius ratio defined by the ratio of

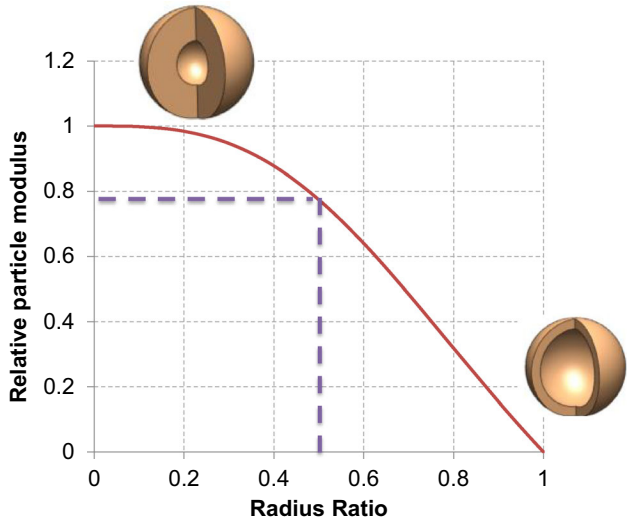

Fig. 9. Relative particle modulus defined by the modulus of a hollow particle divided by the modulus of the particle material. The relative modulus decreases as the wall thickness increases

inner to outer radius of the particle. The relative modulus is calculated by Eq. 8[41]:

$$\frac{E_{mb}}{E_g} = \frac{(1-2V_g)(1-\eta^3)}{(1-2V_g)+\left(\frac{1+V_g}{2}\right)\eta^3}, \quad (8)$$

where v_g and η refer to the Poisson's ratio of particle material and radius ratio of the particle, respectively. Although such a relation for strength is not available for cenospheres because strength has a very strong dependence on the defects, for perfect particles, a decrease in the strength with decreasing wall thickness is expected. Most FA cenospheres used for synthesizing composites can be classified as thick-walled particles (η = 0.6–0.8) compared with engineered glass hollow particles that are mostly in the range η = 0.9–0.98. The considerations illustrated by Fig. 9 are important in deciding the volume fraction of a given particle type in the composite. This figure shows the dependence of the relative particle modulus (effective modulus of hollow particle/modulus of the particle material) on the radius ratio parameter.

An optimum volume fraction can be found for reinforcement in many composite systems. It has been shown that the tensile strength of epoxy filled with FA increases till 6.5 vol.% FA (52 m Nm^{-2}), and further addition of FA resulted in the reduction of tensile strength.[42] Similarly, Rohatgi et al.[43] observed ~ 12% improvement in the compressive yield strength with the addition of 4.9 vol.% FA in epoxy with respect to the unreinforced epoxy. Further addition of FA led to decrease in yield strength up to 19%. Reinforcement of surface-treated FA cenosphere/polyethylene has shown improved mechanical and tribological properties.[35] The composites with 10 wt.%, 15 wt.%, and 20 wt.% FA were prepared by mechanically mixing the

polyethylene granules and FA treated by octadecyltricholorosilane at 160°C using a roll mill. The composite with surface-treated FA showed five to six times higher impact strength than the untreated FA/polyethylene composite. Tribological tests were carried out using pin-on-disk setup against the 400-grit-size abrasive paper. The study observed that the wear rate increases with increase in cenosphere concentration because of filler–filler interaction. However, the study did not compare the wear rate with unreinforced polyethylene to confirm the effectiveness of the cenosphere in polyethylene for tribological applications. Dadkar et al.[44] investigated the tribological performance of the phenolic matrix reinforced with FA and aramid fiber composites for frictional brake application. The observed COF and wear results are shown in Fig. 10. The lowest COF was observed for intermediate amount of FA (Fig. 10a), and the wear also indicates the same trend (Fig. 10b). A summary of the mechanical and tribological performance of polymer-based FA composites is presented in Table IV.

Thermogravimetric analysis shows that the addition of FA in epoxy increases the decomposition temperature. Gu et al.[45] investigated the heat resistance performance of FA/epoxy composite by thermogravimetric analyzer in the temperature range of 200–430°C with 10°C/min heating rate. The initial decomposition temperature was observed to increase with increase in FA content in the epoxy matrix. Epoxy with 70 vol.% FA showed a maximum initial decomposition temperature of 378°C compared with the 321°C of the unreinforced epoxy.

One of the observations from Table IV is that some of the composites show enhanced properties while some other composites show reduced mechanical properties due to FA cenospheres incorporation. This trend is likely due to the hollow structure of the cenospheres. While mechanical properties such as strength and modulus are more than one order of magnitude different for the resin and the oxides that comprise cenospheres, the effective properties of cenospheres depend on their wall thickness and defects present in their shell structure. Due to thin walls and defects, their effective properties may be comparable to those of the matrix resin, and the composite may show a crossover point in the mechanical properties at a certain volume fraction of cenospheres. Testing of single particles of SiC has shown that, despite very high modulus of SiC material, the hollow particles of SiC may have low effective modulus due to the wall-thickness effect and embedded defects,[53] and similar effects are also expected in FA cenospheres. The higher volume fraction of FA particles can lead to increased particle failure due to particle-to-particle interaction effects during composite manufacturing and can yield lower tensile strength. In the case of MMCs, the matrix modulus and strength are either comparable to or higher than those of the cenospheres, which results in different mechanisms for reinforcement in the composite, including some related to precipitate formation, grain refinement, and dislocations. In addition, the properties of PMCs and MMCs are calculated at different strain levels, which also contributes to the mechanism that is dominant in the measured mechanical properties.

Functionally Graded FA/Polymer Composites

The functionally graded composite consists of two or more components with a gradient in composition from one end to another, resulting in respective gradient in properties. Rohatgi et al.[43] utilized the lower density FA cenospheres to synthesize functionally graded polyester/FA composite. In this work, the mixture of cenospheres particles (600 kg/m^3) and polyester resin (1210 kg/m^3) was cast into a glass tube followed by curing for 24 h. The lower density of the particles compared with polyester resin facilitated the rising of the particles in the tube and led to the gradient distribution of particles along the height of the glass tube, as

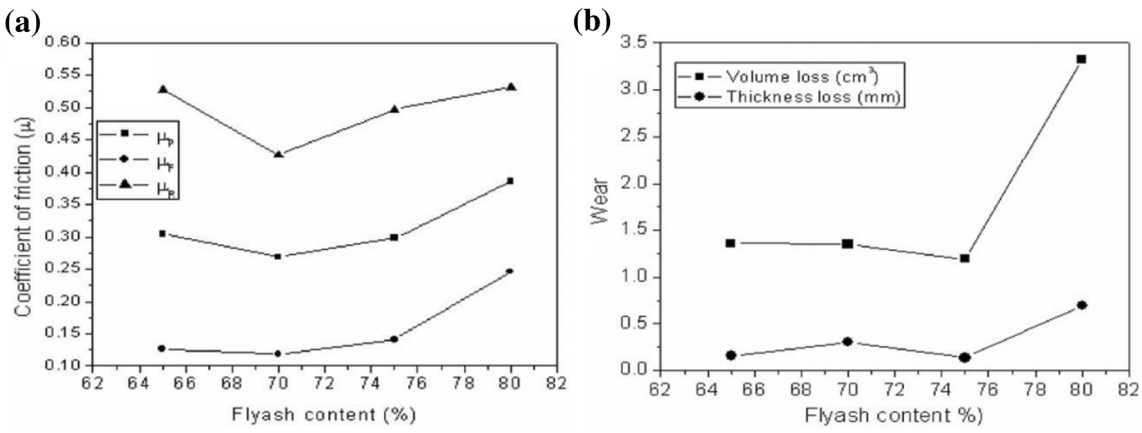

Fig. 10. (a) COF and (b) wear performance of phenolic matrix reinforced with FA and aramid fibers where μ_P (P-performance), μ_F (F-fade), and μ_R (R-recovery). Reprinted with permission from Ref. 44

Table IV. Performance of FA-reinforced polymer matrix composites

Matrix	Reinforcement	Property	References
Epoxy	FA = 10 vol.% (paraffin oil modified)	Compressive strength = 55%, modulus = 58.8%	40
Epoxy	FA = 10 vol.% (Silane modified)	Compressive strength = 43.3%, modulus = 100%	40
Epoxy	FA = 6.5 vol.%	Tensile strength = 8.3%, toughness = 56.2%	42
Phenolic	FA = 70 vol.%	COF = 0.12, wear depth = 0.25 mm	44
Layered structure of epoxy-fiber glass	FA = 10 wt.%	Tensile stress = − 24%, impact strength = − 26.4%	46
Epoxy	FA = 4.9 vol.%	Compressive yield strength = 12%	43
Epoxy	FA = 29.5 vol.%	Compressive yield strength = − 19%	43
Vinyl ester	FA = 60 vol.%	CTE = − 67%, flexural strength = − 73%, flexural modulus = 47%	47
Vinyl ester	FA = 40 vol.%	Compressive strength = − 25%, Compressive modulus = 45%	47
Epoxy	FA = 16 wt.%	Compressive modulus = 68%	48
Epoxy	FA = 10 vol.%	Modulus = 23.5%	49
Epoxy	FA = 10 wt.%	Tensile strength = − 38%, flexural strength = − 12.37%	50
Geopolymer	FA = 48.2 wt.%	Compressive strength = 63%	51
Epoxy	FA = 20 wt.%	Tensile strength = 33.3%	52

shown in Fig. 11a. After casting, the composite was sectioned into specimens with different volume fraction of cenospheres, and their compressive properties were characterized. The maximum compressive yield strength was observed with 4.9 wt.% FA, and then the yield strength decreased with further addition of FA, as shown in Fig. 11b. The decrease in yield strength with further addition of FA was attributed to increased particle-to-particle interaction as the strain increases under compression. The modulus increased with increase in FA because FA particles are stiffer than the matrix. Figure 11c and d show SEM micrographs taken before and after the compressive test for composite with 29.5 vol.% FA, respectively. Multiple cracks around the cenospheres can be observed. These cracks propagated into the matrix and initiated the failure. Qualitatively similar results were obtained in other studies focused on functionally graded cenosphere-filled composites.[48]

CONCLUSION

FA is a waste byproduct that can be used as a filler or reinforcement in metals and polymers to synthesize high-performance composites. The lower cost and density of cenosphere-filled composites as well as the utilization of waste material in their structure make them economically viable and ecofriendly. A few selected studies are described in detail in this review to discuss the trends in properties, while a larger set of studies is tabulated to provide an overview of the field in a concise manner. The uniform dispersion of the FA in Al matrix composites significantly improves their hardness and compressive strength, but sacrifices tensile strength and ductility to some extent. The addition of FA into Al also helps to decrease the CTE. FA/Al alloy composites have shown excellent frictional and wear performance because of harder FA particles that alter the wear mechanisms in comparison with unreinforced Al due to the increase in hardness and reduction in metal-to-metal contact. The hardness increases by 20–40% with addition of 10–40 wt.% FA in Al matrix. The COF decreases from 0.4 to 0.09 as a result of incorporation of 15 wt.% FA in the matrix of Al alloys, whereas the wear resistance has been observed to increase up to 40% with the same amount of FA. Addition of hollow cenospheres of FA can significantly decrease the density of matrices; 65 vol.% incorporation of FA cenospheres decreased the density of Al by 50%. Incorporation of cenospheres in matrices leads to formation of syntactic foams, which enhances the energy absorption efficiency of Al alloy. FA-reinforced metal matrix composites are not suitable for corrosive environments due to their susceptibility to pitting corrosion, where inert FA particles act as initiation sites for pitting.

For polymer matrix composites, surface treatment of FA particles is required to improve the wettability and interaction between FA and polymers. Different surface modifier agents that can improve the mechanical properties are discussed in this article. It is also evident that the FA content in the polymer matrix has to be optimized to achieve the desired properties. Furthermore, the lower density of FA cenospheres makes them floatable on the matrices during processing, leading to formation of functionally gradient microstructures. The

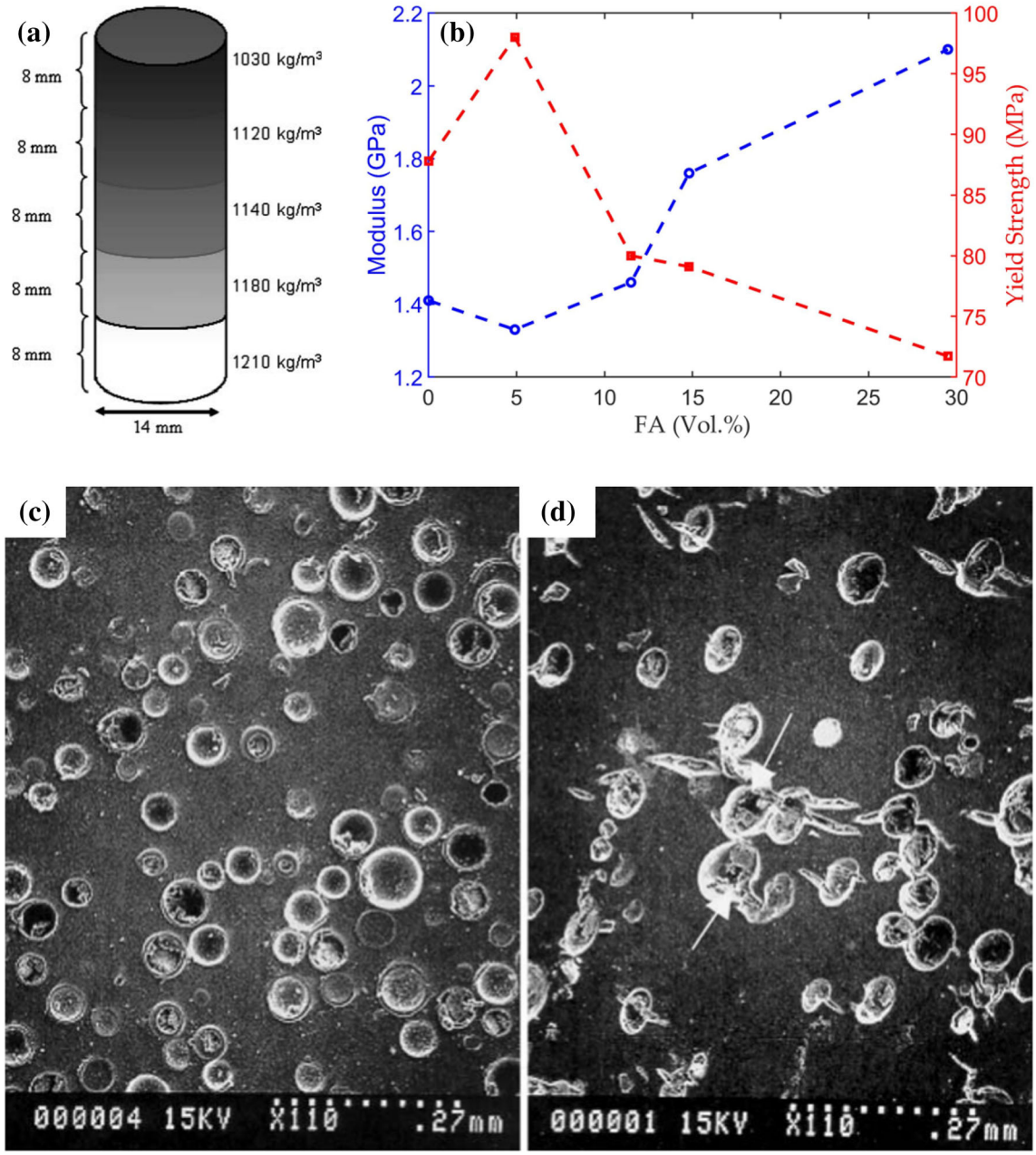

Fig. 11. (a) Schematic of functionally graded polyester/FA composite and (b) variation in compressive yield strength and modulus with FA content; SEM micrographs of 29.5 vol.% FA composite (c) before and (d) after the test. Reprinted with permission from Ref. 43

available tribological studies show that a hybrid composite with solid lubricants and FA polymer matrix composite can be developed with improved tribological performance.

REFERENCES

1. M. Cheriaf, J.C. Rocha, and J. Péra, *Cem. Concr. Res.* 29, 1387 (1999).
2. ASTM C618-19, *Standard Specification for Coal Fly Ash and Raw or Calcined Natural Pozzolan for Use in Concrete* (West Conshohocken: ASTM international, 2010).
3. R. Helmuth, *Fly Ash in Cement and Concrete*. SP040.01T (1987).
4. US Research Nanomaterials, Inc, https://www.us-nano.com/ , Accessed 25 Dec 2019.
5. P.K. Rohatgi, P.L. Menezes, and M.R. Lovell, *Green Tribology*, ed. M. Nosonovsky and B. Bhushan (Springer, Berlin, Heidelberg, 2012), pp. 429–443.
6. J. Voelcker, Green car reports. https://www.greencarreports.com/news/1093560_1-2-billion-vehicles-on-worlds-roads-now-2-billion-by-2035-report. Accessed 24 Dec 2019.
7. P.K. Rohatgi, D. Weiss, and N. Gupta, *JOM* 58, 71 (2006).
8. P. Rohatgi, *JOM* 43, 10 (1991).
9. M. Malaki, W. Xu, A.K. Kasar, P.L. Menezes, H. Dieringa, R.S. Varma, and M. Gupta, *Metals (Basel)* 9, 330 (2019).
10. M.W. Chase Jr, C.A. Davies, J.R. Downey Jr, D.J. Frurip, R.A. McDonald, and A.N. Syverud, *J. Phys. Chem. Ref. Data* 14, 1 (1985).
11. W.M. Haynes, *CRC Handbook of Chemistry and Physics* (Cambridge: CRC, 2014).

12. A.R. Farkoosh and M. Pekguleryuz, *Mater. Sci. Eng. A* 582, 248 (2013).
13. E. Rincón, H.F. López, M.M. Cisneros, H. Mancha, and M.A. Cisneros, *Mater. Sci. Eng. A* 452–453, 682 (2007).
14. A.R. Farkoosh, X.G. Chen, and M. Pekguleryuz, *Mater. Sci. Eng. A* 620, 181 (2015).
15. H.C. Anilkumar, H.S. Hebbar, and K.S. Ravishankar, *Int. J. Mech. Mater. Eng.* 6, 41 (2011).
16. J.D.R. Selvam, D.S. Robinson Smart, and I. Dinaharan, *Mater. Des.* 49, 28 (2013).
17. E. Gikunoo, O. Omotoso, and I.N.A. Oguocha, *Mater. Sci. Technol.* 21, 143 (2005).
18. J. Hashim, L. Looney, and M.S.J. Hashmi, *J. Mater. Process. Technol.* 119, 329 (2001).
19. P.K. Rohatgi, J.K. Kim, N. Gupta, S. Alaraj, and A. Daoud, *Compos. Part A Appl. Sci. Manuf.* 37, 430 (2006).
20. D.D. Luong, N. Gupta, A. Daoud, and P.K. Rohatgi, *JOM* 63, 53 (2011).
21. D.D. Luong, N. Gupta, and P.K. Rohatgi, *JOM* 63, 48 (2011).
22. S.H. Juang and C.-S. Xue, *Mater. Sci. Eng. A* 640, 314 (2015).
23. M.M. Boopathi, K.P. Arulshri, and N. Iyandurai, *Am. J. Appl. Sci.* 10, 219 (2013).
24. S.P. Dwivedi, S. Sharma, and R.K. Mishra, *J. Braz. Soc. Mech. Sci. Eng.* 37, 57 (2015).
25. M. Ramachandra and K. Radhakrishna, *Wear* 262, 1450 (2007).
26. S. Venkat Prasat and R. Subramanian, *Ind. Lubr. Tribol.* 65, 399 (2013).
27. C.S. Ramesh and S.K. Seshadri, *Wear* 255, 893 (2003).
28. J.B. Rao, D.V. Rao, I.N. Murthy, and N. Bhargava, *J. Compos. Mater.* 46, 1393 (2012).
29. A. Mohammed Razzaq, D. Majid, M. Ishak, and U. Basheer, *Metals (Basel)* 7, 477 (2017).
30. V. Mohanavel, S.S. Kumar, R.V. Srinivasan, P. Ganeshan, and K.T. Anand, *J. Chem. Pharm. Sci. ISSN* 974, 2115 (2017).
31. P.K. Rohatgi, N. Gupta, and S. Alaraj, *J. Compos. Mater.* 40, 1163 (2006).
32. K.V.S. Murthy, D.P. Girish, R. Keshavamurthy, T. Varol, and P.G. Koppad, *Prog. Nat. Sci. Mater. Int.* 27, 474 (2017).
33. N. Nagaraj, K.V. Mahendra, and M. Nagaral, *Mater. Today Proc.* 5, 3109 (2018).
34. J. Bienia, M. Walczak, B. Surowska, and J. Sobczaka, *J. Optoelectron. Adv. Mater.* 5, 493 (2003).
35. N. Chand, P. Sharma, and M. Fahim, *Mater. Sci. Eng. A* 527, 5873 (2010).
36. P.K. Rohatgi, N. Gupta, B.F. Schultz, and D.D. Luong, *JOM* 63, 36 (2011).
37. D.D. Luong, O.M. Strbik, V.H. Hammond, N. Gupta, and K. Cho, *J. Alloys Compd.* 550, 412 (2013).
38. B.R.B. Kumar, M. Doddamani, S.E. Zeltmann, N. Gupta, S. Gurupadu, and R.R.N. Sailaja, *J. Mater. Sci.* 51, 3793 (2016).
39. B.R. Bharath Kumar, S.E. Zeltmann, M. Doddamani, N. Gupta, S. Gurupadu, and R.R.N. Sailaja, *J. Appl. Polym. Sci.* 133, 43881 (2016).
40. S.M. Kulkarni and Kishore, *J. Adhes.* 78, 155 (2002).
41. J. Nji and G. Li, *Compos. Part A Appl. Sci. Manuf.* 39, 1404 (2008).
42. V.K. Srivastava and P.S. Shembekar, *J. Mater. Sci.* 25, 3513 (1990).
43. P.K. Rohatgi, T. Matsunaga, and N. Gupta, *J. Mater. Sci.* 44, 1485 (2009).
44. N. Dadkar, B.S. Tomar, and B.K. Satapathy, *Mater. Des.* 30, 4369 (2009).
45. J. Gu, G. Wu, and Q. Zhang, *Mater. Sci. Eng. A* 452–453, 614 (2007).
46. R. Purohit, P. Sahu, R.S. Rana, V. Parashar, and S. Sharma, *Mater. Today Proc.* 4, 3102 (2017).
47. M. Labella, S.E. Zeltmann, V.C. Shunmugasamy, N. Gupta, and P.K. Rohatgi, *Fuel* 121, 240 (2014).
48. M. Doddamani, V.C. Shunmugasamy, N. Gupta, and H.B. Vijayakumar, *Polym. Compos.* 36, 685 (2015).
49. S.M. Kulkarni, *J. Appl. Polym. Sci.* 84, 2404 (2002).
50. C.K. Goh, S.E. Valavan, T.K. Low, and L.H. Tang, *Waste Manag.* 58, 309 (2016).
51. G. Roviello, L. Ricciotti, O. Tarallo, C. Ferone, F. Colangelo, V. Roviello, and R. Cioffi, *Materials (Basel)* 9, 461 (2016).
52. G.K.M. Raju, G.M. Madhu, M.A. Khan, and P.D.S. Reddy, *Mater. Today Proc.* 5, 27998 (2018).
53. V.C. Shunmugasamy, S.E. Zeltmann, N. Gupta, and O.M. Strbik, *JOM* 66, 892 (2014).